



Published in final edited form as:

Curr Opin Neurol. 2011 August ; 24(4): 386–393. doi:10.1097/WCO.0b013e328348972a.

Novel Frontiers in MRI of the brain

Jeff H. Duyn and Alan P. Koretsky

Laboratory of Functional and Molecular Imaging, National Institutes of Neurological Disorders and Stroke, National Institutes of Health, Bethesda, MD 20892

Abstract

Recent developments in the use of MRI contrast in images of the brain continue to expand the use of MRI in neuroscience. Higher magnetic field strengths and innovative ways to manipulate contrast have allowed improved visualization of the various properties of brain tissues, facilitating the anatomical definition of functional areas and their white matter fiber connections. This is bringing us closer to understanding the evolutionary blueprint of the brain, improving the detection and characterization of disease, and help guiding treatment. This review highlights some areas of recent progress, including the application of magnetic susceptibility contrast to study white matter fibers and cortical layers and the use of endogenous and exogenous contrast to study cellular events.

Introduction

Since its introduction into clinical practice in the early eighties, MRI has continued to develop rapidly, and has become the premier clinical tool to study human brain anatomy and function. Major developments have occurred in a number of areas, including sensitivity,

Corresponding author contact information: National Institute of Neurological Disorders and Stroke, National Institutes of Health, 9600 Rockville Pike, Bethesda, MD 20892 koretskya@ninds.nih.gov.

Jananoff dopamine paper Nat Biotech 2010

First demonstration of a MRI contrast agent sensitive to dopamine release from neurons in rats. The agent was produced using state-of-the-art protein evolution techniques.

Masaki PNAS paper 2010

First study demonstrating laminar variation in cortical ferritin content that is detectable with high field MRI

Epilepsy 7T (MGH) Madan 2009

Early clinical application of high field MRI demonstrating the feasibility of accurately localizing seizure focus in cortical dysplasia-induced.

Abosch, Harel, Neurosurgery 2010

Demonstration of improved electrode placement for deep brain stimulation using T2*-weighted imaging at 7T

Summer, Neuroimage 2009

Early work demonstrating that endogenous precursor cells in the rodent can be labeled for MRI by direct injection of iron oxide contrast where the cells arise and the cells can be imaged as they migrate.

Zhang Jacobs, Plos One 2010

Neural tract tracing with manganese enhanced MRI demonstrates that altered circuitry in dopamine transporter knockout mouse model can be efficiently detected.

Assaf, Basser Brain 2009

Demonstration of the possibility of measuring axon diameter with MRI based on restricted water diffusion

Stoll & Bendszus review 2010

Excellent review on MRI approaches using targeted agents and cell tracking to studying inflammation in the brain.

Kang, Int J of Stroke 2010

First demonstration of ability to image the lenticulo-striate arteries with MRI; Indicates the potential clinical value of high field (7T) MRI systems.

spatial resolution, and the type of contrast that can be generated with and without the administration of contrast agents. This has improved the quality of MRI scans and broadened the range of applications in basic neuroscience, pre-clinical models and the diagnosis and management of diseases of the brain.

Early MRI studies had a relatively poor resolution (about 2.5mm) and a limited and poorly understood contrast that was based on the density of water protons and their NMR relaxation times (T_1 and T_2). Early applications included the study of the significant tissue abnormalities occurring in Multiple Sclerosis (MS), stroke, and brain tumors [1,2]. Current MRI technique allow resolutions to 300 μm (75 μm in rodents), and sensitization to a great variety of contrast mechanisms enabling routine measurements of blood flow [3] and deoxyhemoglobin content [4], water diffusion [5], axonal transport [6], and cell migration [7]. Improved resolution and flexibility in contrast are allowing quantitative studies of parcellation of brain into grey and white matter and the architecture of its fiber pathways [6,8] and cortical laminar subdivisions.

Counting lesions in MS with contrast agents that detect blood brain barrier disruption due to inflammation have become a critical part of development of new treatments and monitoring their efficacy. Techniques sensitized to brain blood flow and water diffusion are helping to characterize the severity, extent, and temporal evolution of ischaemic stroke and are impacting treatment protocols [9]. Quantitative anatomy with MRI is leading to assessment of the stage of Alzheimer's Disease (AD), which should greatly decrease the number of patients needed in trials of new therapies[10]. Monitoring temporal variations in blood flow and deoxyhemoglobin content using functional MRI (fMRI) during behavioral tasks is helping to elucidate the brain's functional subdivisions [11] as well as reveal abnormalities in pathological conditions [12]. Diffusion weighted MRI is being used to detect abnormal water mobility in a variety of pathologies including brain tumors, head trauma and inflammatory disease such as meningitis and encephalitis [8]. Lastly, the use of contrast agents such as iron oxide has allowed the tracking of cells during various cellular therapies[7]. The impact of MRI on studies of the brain continues to grow. In this review, we will highlight some of the most recent developments in the areas of structural, cellular, and molecular MRI. Advances in other areas of MRI, such as fMRI, will be discussed in other reviews in this issue.

Resolution and Contrast Improvements in Anatomical MRI

Two important developments over the last decade have substantially improved the sensitivity of brain MRI based on water protons (^1H): high field magnets and array detectors. Modern 7 Tesla scanners with 32-channel array detectors allow a 10–100 fold improvement in sensitivity (i.e. SNR) over early 0.15–1.5 Tesla systems with single channel detectors [13]. This has directly translating into improved resolution for structural MRI. A direct outgrowth of the move to higher field has been the increased use of T_2^* -weighted contrast, which, particularly at high field, is exquisitely sensitive to subtle spatial variations in the magnetic properties of tissues. As will be shown below, T_2^* contrast may be used to investigate the sub-structure of grey and white matter.

Segmentation of Grey and White Matter

The ability to distinguish between the functionally and structurally different tissues of grey and white matter is one of the great strengths of MRI, and has helped detection of and distinction between various disease processes. The MRI acquisition technique of choice has been MPRAGE [14], which is based on T_1 contrast and allows robust grey white matter segmentation. A number of analysis methods rely on such data to generate grey matter surface maps [15], and analyze grey matter volume [16] or local variations in cortical thickness [17], and subtle changes of these due to disease [18]. These methods have been greatly helped by the improvements available with modern MRI array detectors and optimized acquisition [19], allowing resolutions of about 0.5 mm, compared to the $\times 1$ mm resolution available with single channel detectors at 3 T.

Detecting Structure within Grey and White Matter

One exciting development in MRI-based neuroimaging is the possibility of distinguishing cortical layers. Since the early 1900's neuro-anatomists have studied brain samples to investigate whether a cortical region's function is reflected in its cellular structure, including laminar density of cell bodies and myelinated axons [20,21]. MRI studies based on T_1 and proton density contrast have suggested that this is, to some extent, possible in-vivo in humans [22–24] and non-human primates [25,26].

In animal studies use of manganese based contrast has enabled parcellation of a number of grey matter areas as well as detection of the laminar structure of olfactory bulb, cortex, cerebellum, and retina [27–29]. Neural structures as small as glomeruli in the olfactory bulb have been detected with manganese based contrast [30].

Exploiting the strongly increased contrast in T_2^* -weighted images at high field, recent studies have shown improved visualization of layers based on NMR resonance frequency shifts [31,32] (Fig. 1a). This contrast appears to be dominated by local variations in iron stored in ferritin [33], the role of which is still poorly understood (Figs. 1b,c). Despite the problems with quantitative understanding of the contrast, magnitude and phase sensitive T_2^* -weighted MRI at high field is beginning to find widespread application to studying the human brain [32,34–39].

One exciting possibility is that T_2^* weighted MRI may be able to detect the subtle brain changes associated with disease. For example iron-laden plaques associated with AD have been detected in the hippocampus in ex-vivo human tissue [40] and in-vivo in mouse models [41]. In addition, changes in T_2^* relaxation characteristics may be indicative of myelin loss and therefore be valuable in characterizing demyelinating diseases such as MS and Adrenoleukodystrophy (ALD) [42–45]

The Fiber Structure of White Matter

One of the fastest growing fields in MRI is the use of diffusion tensor imaging (DTI) to study brain fiber structure [46], exploiting the fact that water preferentially diffuses along the axonal direction [47,48]. Applied clinically, altered diffusion properties may indicate

compromised fiber structure or cell swelling due to ischemic stroke or inflammation. Although the current resolution is limited to about 2 mm, ongoing developments of high strength gradient systems combined with high field magnets are leading to improvements that will bring the resolution to 1 mm.

DTI data can also be used to track the major fiber pathways in the brain allowing visualization of the connections between cortical areas[49]. This information is increasingly being combined with that from fMRI of task-evoked and spontaneous activity to study brain connectivity [50].

Recent work has indicated that fiber bundles can also be visualized with T_2^* weighted MRI [31], as both T_2^* and resonance frequency shifts appear to depend on fiber properties, including orientation [51,52] and potentially myelin density [53] (Fig. 2). The orientation dependence may originate from magnetic susceptibility anisotropy [52,54] and anisotropically distributed field perturbers [55] and may allow a spatial resolution superior to DTI: for example small bundles like the mamillo-thalamic tract can be readily visualized with phase images [31]. However, full characterization of the brain's fiber bundles with T_2^* contrast may be less practical than with DTI as it will require data acquired at multiple head orientations relative to the magnetic field, or alternatively sophisticated processing methods [56]. Therefore, this type of data is likely to complement rather than replace information gathered with DTI.

Direct Neuronal Tract Tracing with MRI

DTI enables following major white matter tracts and much work is ongoing to begin to use this to measure connections between areas of the brain. An alternative approach that has found widespread use in animal models is to directly inject an MRI contrast agent into an area of the brain that can trace neuronal connections. Most useful has been Mn^{2+} which is transported in an anterograde direction between grey matter areas and can cross synapses, allowing mapping of poly-synaptic connections [57–60]. It has been shown that with proper timing, Mn^{2+} can be used to trace neural connections at the level of specific laminar inputs [61]. There have been numerous applications of Manganese Enhanced MRI for neuronal tract tracing in animal models including studies of plasticity associated with learning, stroke, and Parkinson's Disease [62–64] and for assessing the extent of neural damage along the optic nerve and spinal chord [65]. The mechanism of entry of Mn^{2+} into neurons and subsequent neuronal transport is not fully understood. Studies using mouse mutants and ion channel inhibitors is beginning to lead to some understanding [66]. The widespread use of Manganese Enhanced MRI for neuronal tracing is leading to work to develop other MRI agents for tracing. A classical neuronal tracer, cholera toxin B (CTB), was linked with a Gadolinium (Gd) chelate which enabled MRI detection of neuronal connections [67]). An advantage is that CTB does not cross synapses and allows mapping of mono-synaptic connections.

Vascular MRI

An area that has made much progress recently is vascular MRI. There is a long tradition in using MRI to perform angiography, typically using contrast agents to highlight the

vasculature [68]. Detection of vessels at high magnetic fields greatly improves the visualization of arteries and veins due to increases in T_1 and T_2^* -based vascular contrast coupled with sensitivity gains. Resolutions on the order of 0.35 mm are being obtained without exogenous contrast agents [69,70]. This is allowing the detection of small vessel such as the lenticulo-striate arteries [70], and veins within MS lesions [71,72], and is expected to improve the detection of vascular abnormalities in brain tumors and the detection of micro bleeds resulting from brain trauma.

A key development in MRI was the introduction of Gd chelates as effective T_1 contrast agents. The greatest impact has been on imaging disruption of the blood-brain barrier due to inflammation. Quantitative modeling of Gd leakage [68] is being used to assess tumor vasculature [73]. Recently, leakage of Gd into brain has been detected after thrombolytic therapy in stroke thanks to higher sensitivity MRI using array coils [74]. This phenomenon may be used to guide future therapeutic protocols.

Development of novel molecular imaging agents targeted to the brain vasculature is a fertile area of work. MRI contrast agents that bind specifically to blood clots [75], and targeted MRI contrast using endothelial adhesion molecules has been demonstrated in animal models [76]. This work is important for understanding pathophysiology in animal models. The translation to human remains a very significant challenge with any new MRI agent. Simple Gd chelates remain the only widely used MRI contrast agents used to study brain vasculature in humans.

Novel MRI Techniques to Increase Sensitivity

There is growing interest in using new agents in MRI to perform molecular imaging of specific biological species or cellular processes. A general difficulty with these methods is their low sensitivity, requiring many micromolar to millimolar levels of agents. A number of directions are being explored to increase sensitivity to specific agents. It has long been known that magnetization transfer can be used to detect small pools via exchange with water. So called “CEST” techniques are being used to produce novel contrast agents [77,78]. Endogenous molecules can be detected with CEST contrast using the specific saturation of amide protons on mobile lipids and proteins [79]. This has been applied to measuring pH and for discriminating brain tumors from radiation necrosis [80]. Expression of high levels of peptides that are efficient CEST agents can be used to monitor gene expression [81].

MRI of nuclei other than protons, such as ^{31}P or ^{13}C has been successfully used for many years to provide molecular and biochemical information that may not be accessible with ^1H MRI [82]. MRI of other nuclei is hampered by low sensitivity, which has prevented widespread application. The recent introduction of hyper-polarization techniques to greatly increase the signal especially of ^{13}C containing molecules holds much promise to overcome this problem [83].

Cellular Imaging

With the increasing use of stem cells and induced pluripotent cells to treat diseases of the brain and spinal chord it will become very important to develop MRI techniques to monitor

the fate of transplanted cells. Over the past twenty years there has been a steady development of tools to enable cellular imaging with MRI. Most of this relies on loading cells with exogenous contrast agents such as iron oxide nanoparticles [84–88]. There have been provocative studies that indicate MRI might be able to detect neural precursor cells in the normal human brain using MRI [89,90], and MRS [91] without exogenous contrast. However, none of these approaches has found widespread use as yet and the majority of work tracking cells with MRI relies on loading cells with enough contrast agent to enable detection.

Most MRI studies imaging of transplanted cells have used dextran coated iron oxide particles that are very strong T_2^* agents, combined with a variety of techniques to get efficient cell labeling [85,86,92,93]. If enough iron oxide nanoparticles can be gotten into cells, it is possible to detect single cells in animals with MRI [85,94-96]. Rather than nanoparticles, micron sized particles of iron oxide are also being used because a single such particle contains enough iron oxide to be detectable [95]. This has enabled the tracking of neural progenitors into the olfactory bulb in the rodent brain after direct injection of particles near the sub-ventricular zone where these cells originate [97–99, Fig. 2].

An interesting new development is the micro-fabrication of contrast agent particles, by which their magnetic properties can be accurately controlled. This has allowed distinguishing multiple particles within MRI [100,101], analogous to having different colors in fluorescence based imaging. Such an approach has the potential to enable the separation of different types of cells.

Several other materials/compounds have been used for cell tracking, including GadoFluorine [102], manganese based particles [103], carbon nanotubes [104,105]), CoPt particles[106]. Particles made from ^{19}F labeled emulsions have been successfully used to label immune cells [105,107,108] with the advantage that there is no background signal from water, allowing specific detection of the ^{19}F label.

Cellular Imaging Applications

There are two major classes of cell labeling experiments that are finding widespread use. The first one is based on intravenous injection of iron oxide which is taken up by resident macrophages in a tissue. A number of diseases lead to increased tissue macrophage content and this approach allows visualization with MRI. Organ rejection [109], and inflammation due to various pathologies including ischemia in kidney [110], and experimental allergic encephalitis [111] have been studied in animal models using direct injection of iron oxide into the circulation (for review see [88,112]). Several studies indicate that this approach will be useful for translation to humans [113,114]. A significant problem is producing safe iron oxide formulations that are efficiently taken up by resident macrophages for human use.

The second class of cell tracking experiment is to take cells in culture, preload them with iron oxide or other suitable contrast and then transplant or inject them into animals. Immune cells [115], tumor cells [116], and a number of stem cells [93,97–99] have been studied in this way in animal models. A wide variety of disease models are being studied. It is possible to use MRI both to track cells and to phenotype the tissue using more standard contrast to

determine if the cells are having their desired effects [86]. There are now a few studies in humans that indicate this strategy to label cells ex-vivo and use MRI to follow the cells after transplantation will work. Studies following neural stem cells in the human brain [89], CD34+ cells injected into human spinal chord [90], and dendritic cells injected into human lymph nodes [117] clearly demonstrate the potential. A major hurdle to overcome is the fact that the label is not cell autonomous and the iron oxide can be transferred to cells other than the original labeled cell. For example, cell death would be expected to lead to uptake of the MRI contrast into macrophages or microglial cells. Nonetheless, techniques to track cells in humans, will grow in importance as the number of cell therapies continues to expand.

Summary and Outlook

Improvements in hardware and novel use of contrast continue to transform the ways that MRI can be used to study the brain. In humans, subtle anatomical variations on the scale of about 300 μm can be visualized based on the tissue's magnetic properties, and even higher resolutions are expected based on ongoing hardware improvements. It is anticipated that this will allow the robust visualization of cortical layers, sub-millimeter white matter fiber bundles, and vascular detail. This in turn should further facilitate the identification of brain variations associated with diseases such as AD [35,118], MS [34,38], and epilepsy [37].

In preclinical models there is a rapidly growing list of targeted contrast agents, cell tracking agents, and agents sensitive to brain function that attempt to measure calcium and neurotransmitter levels [119,120]. A few of these agents are becoming routinely used to study a large number of animal models of brain pathology. The translation to human use remains a major hurdle but there are indications that this gap will be filled over the coming decade [89,90,117]. Since the invention of MRI in 1974 by Paul Lauterbur, it has grown to its present central role in human brain imaging. The new developments taking place make the future bright for continued progress.

References

1. Young IR, Hall AS, Pallis CA, Legg NJ, Bydder GM, Steiner RE. Nuclear magnetic resonance imaging of the brain in multiple sclerosis. *Lancet*. 1981; 2(8255):1063–1066. [PubMed: 6118521]
2. Bydder GM, Steiner RE, Young IR, Hall AS, Thomas DJ, Marshall J, Pallis CA, Legg NJ. Clinical nmr imaging of the brain. 140 cases. *AJR Am J Roentgenol*. 1982; 139(2):215–236. [PubMed: 6979874]
3. Williams DS, Detre JA, Leigh JS, Koretsky AP. Magnetic resonance imaging of perfusion using spin inversion of arterial water. *Proc Natl Acad Sci USA*. 1992; 89(1):212–216. [PubMed: 1729691]
4. Ogawa S, Lee TM, Nayak AS, Glynn P. Oxygenation-sensitive contrast in magnetic resonance image of rodent brain at high magnetic fields. *Magn Reson Med*. 1990; 14(1):68–78. [PubMed: 2161986]
5. Le Bihan D. Looking into the functional architecture of the brain with diffusion mri. *Nat Rev Neurosci*. 2003; 4(6):469–480. [PubMed: 12778119]
6. Lee JH, Koretsky AP. Manganese enhanced magnetic resonance imaging. *Curr Pharm Biotechnol*. 2004; 5(6):529–537. [PubMed: 15579042]
7. Long CM, Bulte JW. In vivo tracking of cellular therapeutics using magnetic resonance imaging. *Expert Opin Biol Ther*. 2009; 9(3):293–306. [PubMed: 19216619]

8. Nucifora PG, Verma R, Lee SK, Melhem ER. Diffusion-tensor mr imaging and tractography. Exploring brain microstructure and connectivity. *Radiology*. 2007; 245(2):367–384. [PubMed: 17940300]
9. Ostergaard L, Jonsdottir KY, Mouridsen K. Predicting tissue outcome in stroke. *New approaches. Curr Opin Neurol*. 2009; 22(1):54–59. [PubMed: 19155762]
10. Hua X, Lee S, Hibar DP, Yanovsky I, Leow AD, Toga AW, Jack CR Jr, Bernstein MA, Reiman EM, Harvey DJ, Kornak J, et al. Mapping alzheimer's disease progression in 1309 mri scans. Power estimates for different inter-scan intervals. *Neuroimage*. 2010; 51(1):63–75. [PubMed: 20139010]
11. Friston KJ. Models of brain function in neuroimaging. *Annu Rev Psychol*. 2005; 56:57–87. [PubMed: 15709929]
12. Matthews PM, Honey GD, Bullmore ET. Applications of fmri in translational medicine and clinical practice. *Nat Rev Neurosci*. 2006; 7(9):732–744. [PubMed: 16924262]
13. de Zwart JA, Ledden PJ, Kellman P, van Gelderen P, Duyn JH. Design of a sense-optimized high-sensitivity mri receive coil for brain imaging. *Magn Reson Med*. 2002; 47(6):1218–1227. [PubMed: 12111969]
14. Mugler JP 3rd, Brookeman JR. Three-dimensional magnetization-prepared rapid gradient-echo imaging (3d mp rage). *Magn Reson Med*. 1990; 15(1):152–157. [PubMed: 2374495]
15. Van Essen DC, Lewis JW, Drury HA, Hadjikhani N, Tootell RB, Bakircioglu M, Miller MI. Mapping visual cortex in monkeys and humans using surface-based atlases. *Vision Res*. 2001; 41(10–11):1359–1378. [PubMed: 11322980]
16. Ashburner J, Friston KJ. Voxel-based morphometry--the methods. *Neuroimage*. 2000; 11(6 Pt 1): 805–821. [PubMed: 10860804]
17. Fischl B, Dale AM. Measuring the thickness of the human cerebral cortex from magnetic resonance images. *Proc Natl Acad Sci U S A*. 2000; 97(20):11050–11055. [PubMed: 10984517]
18. Lerch JP, Pruessner JC, Zijdenbos A, Hampel H, Teipel SJ, Evans AC. Focal decline of cortical thickness in alzheimer's disease identified by computational neuroanatomy. *Cereb Cortex*. 2005; 15(7):995–1001. [PubMed: 15537673]
19. Van Gelderen P.; Koretsky, AP.; de Zwart, JA.; Duyn, JH. A simple b1 correction method for high resolution neuroimaging. *Proceedings 14th scientific meeting ISMRM; Seattle, WA*. 2006. p. 2355
20. Brodmann, K. *Vergleichende lokalisationlehre der grosshirnrinde*. Leipzig: Barth-Verlag; 1909.
21. Vogt O. Die myeloarchitektonik des isocortex parietalis. *J Psychol Neurol*. 1911; 18:107–118.
22. Clark VP, Courchesne E, Grafte M. In vivo myeloarchitectonic analysis of human striate and extrastriate cortex using magnetic resonance imaging. *Cereb Cortex*. 1992; 2(5):417–424. [PubMed: 1422094]
23. Barbier EL, Marrett S, Danek A, Vortmeyer A, van Gelderen P, Duyn J, Bandettini P, Grafman J, Koretsky AP. Imaging cortical anatomy by high-resolution mr at 3.0t: Detection of the stripe of gennari in visual area 17. *Magn Reson Med*. 2002; 48(4):735–738. [PubMed: 12353293]
24. Bridge H, Clare S, Jenkinson M, Jezzard P, Parker AJ, Matthews PM. Independent anatomical and functional measures of the v1/v2 boundary in human visual cortex. *J Vis*. 2005; 5(2):93–102. [PubMed: 15831070]
25. Bock NA, Kocharyan A, Liu JV, Silva AC. Visualizing the entire cortical myelination pattern in marmosets with magnetic resonance imaging. *J Neurosci Methods*. 2009; 185(1):15–22. [PubMed: 19737577]
26. Pfeuffer J, Merkle H, Beyerlein M, Steudel T, Logothetis NK. Anatomical and functional mr imaging in the macaque monkey using a vertical large-bore 7 tesla setup. *Magn Reson Imaging*. 2004; 22(10):1343–1359. [PubMed: 15707785]
27. Aoki I, Wu YJ, Silva AC, Lynch RM, Koretsky AP. In vivo detection of neuroarchitecture in the rodent brain using manganese-enhanced mri. *Neuroimage*. 2004; 22(3):1046–1059. [PubMed: 15219577]
28. Silva AC, Lee J, Wu CH, Tucciarone J, Pelled G, Aoki I, Koretsky AP. Detection of cortical laminar architecture using manganese enhanced mri. *J Neurosc Meth*. 2007 (in press).

29. Berkowitz BA, Roberts R, Goebel DJ, Luan H. Noninvasive and simultaneous imaging of layer-specific retinal functional adaptation by manganese-enhanced mri. *Invest Ophthalmol Vis Sci*. 2006; 47(6):2668–2674. [PubMed: 16723485]
30. Chuang KH, Belluscio L, Koretsky AP. In vivo detection of individual glomeruli in the rodent olfactory bulb using manganese enhanced mri. *Neuroimage*. 2010; 49(2):1350–1356. [PubMed: 19800011]
31. Duyn JH, van Gelderen P, Li TQ, de Zwart JA, Koretsky AP, Fukunaga M. High-field mri of brain cortical substructure based on signal phase. *Proc Natl Acad Sci U S A*. 2007; 104(28):11796–11801. [PubMed: 17586684]
32. Marques JP, van der Zwaag W, Granziera C, Krueger G, Gruetter R. Cerebellar cortical layers. In vivo visualization with structural high-field-strength mr imaging. *Radiology*. 2010; 254(3):942–948. [PubMed: 20177104]
33. Fukunaga M, Li TQ, van Gelderen P, de Zwart JA, Shmueli K, Yao B, Lee J, Maric D, Aronova MA, Zhang G, Leapman RD, et al. Layer-specific variation of iron content in cerebral cortex as a source of mri contrast. *Proc Natl Acad Sci U S A*. 2010; 107(8):3834–3839. [PubMed: 20133720]
34. Ge Y, Zohrabian VM, Grossman RI. Seven-tesla magnetic resonance imaging. New vision of microvascular abnormalities in multiple sclerosis. *Arch Neurol*. 2008; 65(6):812–816. [PubMed: 18541803]
35. Kerchner GA, Hess CP, Hammond-Rosenbluth KE, Xu D, Rabinovici GD, Kelley DA, Vigneron DB, Nelson SJ, Miller BL. Hippocampal ca1 apical neuropil atrophy in mild alzheimer disease visualized with 7-t mri. *Neurology*. 2010; 75(15):1381–1387. [PubMed: 20938031]
36. Pohmann R, Budde J, Auerbach EJ, Adriany G, Ugurbil K. Theoretical and experimental evaluation of continuous arterial spin labeling techniques. *Magn Reson Med*. 2010; 63(2):438–446. [PubMed: 20024952]
37. Madan N, Grant PE. New directions in clinical imaging of cortical dysplasias. *Epilepsia*. 2009; 50(Suppl 9):9–18. [PubMed: 19761449]
38. Tallantyre EC, Morgan PS, Dixon JE, Al-Radaideh A, Brookes MJ, Morris PG, Evangelou N. 3 tesla and 7 tesla mri of multiple sclerosis cortical lesions. *J Magn Reson Imaging*. 2010; 32(4):971–977. [PubMed: 20882628]
39. Abosch A, Yacoub E, Ugurbil K, Harel N. An assessment of current brain targets for deep brain stimulation surgery with susceptibility-weighted imaging at 7 tesla. *Neurosurgery*. 2010; 67(6):1745–1756. discussion 1756. [PubMed: 21107206]
40. Benveniste H, Ma Y, Dhawan J, Gifford A, Smith SD, Feinstein I, Du C, Grant SC, Hof PR. Anatomical and functional phenotyping of mice models of alzheimer's disease by mr microscopy. *Ann N Y Acad Sci*. 2007; 1097:12–29. [PubMed: 17413006]
41. Jack CR Jr, Marjanska M, Wengenack TM, Reyes DA, Curran GL, Lin J, Preboske GM, Poduslo JF, Garwood M. Magnetic resonance imaging of alzheimer's pathology in the brains of living transgenic mice. A new tool in alzheimer's disease research. *Neuroscientist*. 2007; 13(1):38–48. [PubMed: 17229974]
42. Laule C, Vavasour IM, Kolind SH, Li DK, Traboulsee TL, Moore GR, MacKay AL. Magnetic resonance imaging of myelin. *Neurotherapeutics*. 2007; 4(3):460–484. [PubMed: 17599712]
43. Hwang D, Kim DH, Du YP. In vivo multi-slice mapping of myelin water content using t_2^* decay. *Neuroimage*. 2010; 52(1):198–204. [PubMed: 20398770]
44. Deoni SC. Magnetic resonance relaxation and quantitative measurement in the brain. *Methods Mol Biol*. 2011; 711:65–108. [PubMed: 21279598]
45. van Gelderen P, de Zwart JA, Lee J, Sati P, Reich D, Duyn JH. Non-exponential t_2^* decay in white matter. *Magn Reson Med*. 2011 in press.
46. Bassler PJ, Mattiello J, LeBihan D. Mr diffusion tensor spectroscopy and imaging. *Biophys J*. 1994; 66(1):259–267. [PubMed: 8130344]
47. Moseley ME, Cohen Y, Kucharczyk J, Mintorovitch J, Asgari HS, Wendland MF, Tsuruda J, Norman D. Diffusion-weighted mr imaging of anisotropic water diffusion in cat central nervous system. *Radiology*. 1990; 176(2):439–445. [PubMed: 2367658]
48. Le Bihan D. Molecular diffusion nuclear magnetic resonance imaging. *Magn Reson Q*. 1991; 7(1):1–30. [PubMed: 2043461]

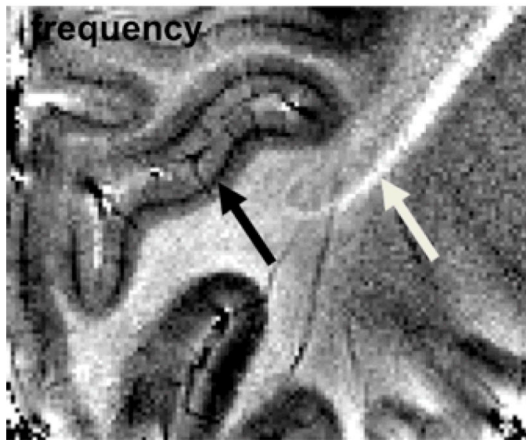
49. Mori S, Zhang J. Principles of diffusion tensor imaging and its applications to basic neuroscience research. *Neuron*. 2006; 51(5):527–539. [PubMed: 16950152]
50. Honey CJ, Thivierge JP, Sporns O. Can structure predict function in the human brain? *Neuroimage*. 2010; 52(3):766–776. [PubMed: 20116438]
51. Wiggins CJ, Gudmundsdottir V, Le Bihan D, Lebon V, Chaumeil M. Orientation dependence of white matter t2* contrast at 7t: A direct demonstration. *Proc Soc Magn Magn Reson Med*. 2008:237.
52. Lee J, Shmueli K, Fukunaga M, van Gelderen P, Merkle H, Silva AC, Duyn JH. Sensitivity of mri resonance frequency to the orientation of brain tissue microstructure. *Proc Natl Acad Sci U S A*. 2010; 107(11):5130–5135. [PubMed: 20202922]
53. Li TQ, Yao B, van Gelderen P, Merkle H, Dodd S, Talagala L, Koretsky AP, Duyn J. Characterization of t(2)* heterogeneity in human brain white matter. *Magn Reson Med*. 2009; 62(6):1652–1657. [PubMed: 19859939]
54. Liu C. Susceptibility tensor imaging. *Magn Reson Med*. 2010; 63(6):1471–1477. [PubMed: 20512849]
55. He X, Yablonskiy DA. Biophysical mechanisms of phase contrast in gradient echo mri. *Proc Natl Acad Sci U S A*. 2009; 106(32):13558–13563. [PubMed: 19628691]
56. Wharton S, Bowtell R. Whole-brain susceptibility mapping at high field. A comparison of multiple- and single-orientation methods. *Neuroimage*. 2010; 53(2):515–525. [PubMed: 20615474]
57. Pautler RG, Silva AC, Koretsky AP. In vivo neuronal tract tracing using manganese-enhanced magnetic resonance imaging. *Magn Reson Med*. 1998; 40(5):740–748. [PubMed: 9797158]
58. Van der Linden A, Verhoye M, Van Meir V, Tindemans I, Eens M, Absil P, Balthazart J. In vivo manganese-enhanced magnetic resonance imaging reveals connections and functional properties of the songbird vocal control system. *Neuroscience*. 2002; 112(2):467–474. [PubMed: 12044464]
59. Saleem KS, Pauls JM, Augath M, Trinath T, Prause BA, Hashikawa T, Logothetis NK. Magnetic resonance imaging of neuronal connections in the macaque monkey. *Neuron*. 2002; 34(5):685–700. [PubMed: 12062017]
60. Zhang X, Bearer EL, Boulat B, Hall FS, Uhl GR, Jacobs RE. Altered neurocircuitry in the dopamine transporter knockout mouse brain. *PLoS One*. 2010; 5(7):e11506. [PubMed: 20634895]
61. Tucciarone J, Chuang KH, Dodd SJ, Silva A, Pelled G, Koretsky AP. Layer specific tracing of corticocortical and thalamocortical connectivity in the rodent using manganese enhanced mri. *Neuroimage*. 2009; 44(3):923–931. [PubMed: 18755280]
62. Van der Linden A, Van Meir V, Boumans T, Poirier C, Balthazart J. Mri in small brains displaying extensive plasticity. *Trends Neurosci*. 2009; 32(5):257–266. [PubMed: 19307029]
63. van der Zijden JP, Wu O, van der Toorn A, Roeling TP, Bleys RL, Dijkhuizen RM. Changes in neuronal connectivity after stroke in rats as studied by serial manganese-enhanced mri. *Neuroimage*. 2007; 34(4):1650–1657. [PubMed: 17175175]
64. Pelled G, Chuang KH, Dodd SJ, Koretsky AP. Functional mri detection of bilateral cortical reorganization in the rodent brain following peripheral nerve deafferentation. *Neuroimage*. 2007; 37(1):262–273. [PubMed: 17544301]
65. Martirosyan NL, Bennett KM, Theodore N, Preul MC. Manganese-enhanced magnetic resonance imaging in experimental spinal cord injury. Correlation between t1-weighted changes and mn(2+) concentrations. *Neurosurgery*. 2010; 66(1):131–136. [PubMed: 20023543]
66. Berkowitz BA, Roberts R, Oleske DA, Chang M, Schafer S, Bissig D, Gadianu M. Quantitative mapping of ion channel regulation by visual cycle activity in rodent photoreceptors in vivo. *Invest Ophthalmol Vis Sci*. 2009; 50(4):1880–1885. [PubMed: 19060264]
67. Wu CW-H, Vasalately O, Wu H, Liu N, Chen D-Y, Koretsky AP, Griffiths G, Tootell RBH, Ungerleider LG. Tracing neuroanatomical connections in-vivo using a novel mr-visualizable compound. *Neuron*. 2011 (in press).
68. Summers PE, Jarosz JM, Markus H. Mr angiography in cerebrovascular disease. *Clin Radiol*. 2001; 56(6):437–456. [PubMed: 11428794]

69. Deistung A, Rauscher A, Sedlacik J, Stadler J, Witoszynskij S, Reichenbach JR. Susceptibility weighted imaging at ultra high magnetic field strengths. Theoretical considerations and experimental results. *Magn Reson Med*. 2008; 60(5):1155–1168. [PubMed: 18956467]
70. Kang CK, Park CA, Park CW, Lee YB, Cho ZH, Kim YB. Lenticulostriate arteries in chronic stroke patients visualised by 7 t magnetic resonance angiography. *Int J Stroke*. 2010; 5(5):374–380. [PubMed: 20854620]
71. Tallantyre EC, Brookes MJ, Dixon JE, Morgan PS, Evangelou N, Morris PG. Demonstrating the perivascular distribution of ms lesions in vivo with 7-tesla mri. *Neurology*. 2008; 70(22):2076–2078. [PubMed: 18505982]
72. Tallantyre EC, Morgan PS, Dixon JE, Al-Radaideh A, Brookes MJ, Evangelou N, Morris PG. A comparison of 3t and 7t in the detection of small parenchymal veins within ms lesions. *Invest Radiol*. 2009; 44(9):491–494. [PubMed: 19652606]
73. Li X, Rooney WD, Varallyay CG, Gahramanov S, Muldoon LL, Goodman JA, Tagge IJ, Selzer AH, Pike MM, Neuwelt EA, Springer CS Jr. Dynamic-contrast-enhanced-mri with extravasating contrast reagent. Rat cerebral glioma blood volume determination. *J Magn Reson*. 2010; 206(2):190–199. [PubMed: 20674422]
74. Kidwell CS, Latour L, Saver JL, Alger JR, Starkman S, Duckwiler G, Jahan R, Vinuela F, Kang DW, Warach S. Thrombolytic toxicity. Blood brain barrier disruption in human ischemic stroke. *Cerebrovasc Dis*. 2008; 25(4):338–343. [PubMed: 18303253]
75. Uppal R, Ay I, Dai G, Kim YR, Sorensen AG, Caravan P. Molecular mri of intracranial thrombus in a rat ischemic stroke model. *Stroke*. 2010; 41(6):1271–1277. [PubMed: 20395615]
76. McAteer MA, Akhtar AM, von Zur Muhlen C, Choudhury RP. An approach to molecular imaging of atherosclerosis, thrombosis, and vascular inflammation using microparticles of iron oxide. *Atherosclerosis*. 2010; 209(1):18–27. [PubMed: 19883911]
77. Ward KM, Aletras AH, Balaban RS. A new class of contrast agents for mri based on proton chemical exchange dependent saturation transfer (cest). *J Magn Reson*. 2000; 143(1):79–87. [PubMed: 10698648]
78. Zhang S, Winter P, Wu K, Sherry AD. A novel europium(iii)-based mri contrast agent. *J Am Chem Soc*. 2001; 123(7):1517–1518. [PubMed: 11456734]
79. Goffeney N, Bulte JW, Duyn J, Bryant LH Jr, van Zijl PC. Sensitive nmr detection of cationic-polymer-based gene delivery systems using saturation transfer via proton exchange. *J Am Chem Soc*. 2001; 123(35):8628–8629. [PubMed: 11525684]
80. Zhou J, Tryggstad E, Wen Z, Lal B, Zhou T, Grossman R, Wang S, Yan K, Fu DX, Ford E, Tyler B, et al. Differentiation between glioma and radiation necrosis using molecular magnetic resonance imaging of endogenous proteins and peptides. *Nat Med*. 2011; 17(1):130–134. [PubMed: 21170048]
81. Gilad AA, McMahon MT, Walczak P, Winnard PT Jr, Raman V, van Laarhoven HW, Skoglund CM, Bulte JW, van Zijl PC. Artificial reporter gene providing mri contrast based on proton exchange. *Nat Biotechnol*. 2007; 25(2):217–219. [PubMed: 17259977]
82. Prost RW. Magnetic resonance spectroscopy. *Med Phys*. 2008; 35(10):4530–4544. [PubMed: 18975700]
83. Day SE, Kettunen MI, Gallagher FA, Hu DE, Lerche M, Wolber J, Golman K, Ardenkjaer-Larsen JH, Brindle KM. Detecting tumor response to treatment using hyperpolarized ¹³c magnetic resonance imaging and spectroscopy. *Nat Med*. 2007; 13(11):1382–1387. [PubMed: 17965722]
84. Mendonca Dias MH, Lauterbur PC. Ferromagnetic particles as contrast agents for magnetic resonance imaging of liver and spleen. *Magn Reson Med*. 1986; 3(2):328–330. [PubMed: 3713497]
85. Yeh TC, Zhang W, Ildstad ST, Ho C. Intracellular labeling of t-cells with superparamagnetic contrast agents. *Magn Reson Med*. 1993; 30(5):617–625. [PubMed: 8259062]
86. Bulte JW, Zhang S, van Gelderen P, Herynek V, Jordan EK, Duncan ID, Frank JA. Neurotransplantation of magnetically labeled oligodendrocyte progenitors. Magnetic resonance tracking of cell migration and myelination. *Proc Natl Acad Sci U S A*. 1999; 96(26):15256–15261. [PubMed: 10611372]

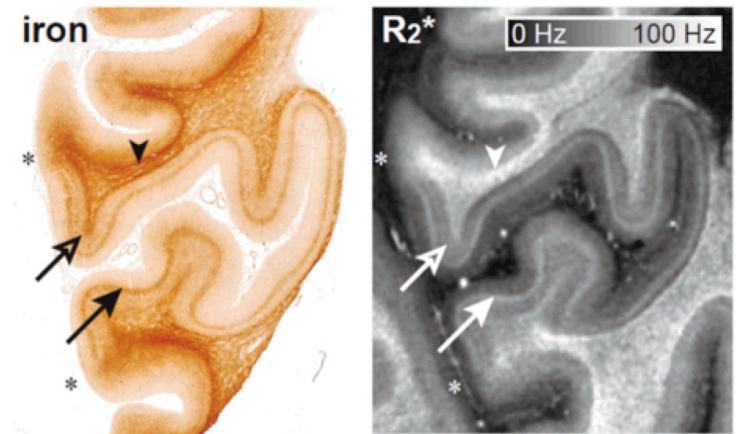
87. Weissleder R, Cheng HC, Bogdanova A, Bogdanov A Jr. Magnetically labeled cells can be detected by mr imaging. *J Magn Reson Imaging*. 1997; 7(1):258–263. [PubMed: 9039625]
88. Weinstein JS, Varallyay CG, Dosa E, Gahramanov S, Hamilton B, Rooney WD, Muldoon LL, Neuwelt EA. Superparamagnetic iron oxide nanoparticles. Diagnostic magnetic resonance imaging and potential therapeutic applications in neurooncology and central nervous system inflammatory pathologies, a review. *J Cereb Blood Flow Metab*. 2010; 30(1):15–35. [PubMed: 19756021]
89. Zhu J, Zhou L, XingWu F. Tracking neural stem cells in patients with brain trauma. *N Engl J Med*. 2006; 355(22):2376–2378. [PubMed: 17135597]
90. Callera F, de Melo CM. Magnetic resonance tracking of magnetically labeled autologous bone marrow cd34+ cells transplanted into the spinal cord via lumbar puncture technique in patients with chronic spinal cord injury. Cd34+ cells' migration into the injured site. *Stem Cells Dev*. 2007; 16(3):461–466. [PubMed: 17610376]
91. Manganas LN, Zhang X, Li Y, Hazel RD, Smith SD, Wagshul ME, Henn F, Benveniste H, Djuric PM, Enikolopov G, Maletic-Savatic M. Magnetic resonance spectroscopy identifies neural progenitor cells in the live human brain. *Science*. 2007; 5852; 318:980–985. [PubMed: 17991865]
92. Frank JA, Miller BR, Arbab AS, Zywicke HA, Jordan EK, Lewis BK, Bryant LH Jr, Bulte JW. Clinically applicable labeling of mammalian and stem cells by combining superparamagnetic iron oxides and transfection agents. *Radiology*. 2003; 228(2):480–487. [PubMed: 12819345]
93. Hoehn M, Kustermann E, Blunk J, Wiedermann D, Trapp T, Wecker S, Focking M, Arnold H, Hescheler J, Fleischmann BK, Schwindt W, et al. Monitoring of implanted stem cell migration in vivo. A highly resolved in vivo magnetic resonance imaging investigation of experimental stroke in rat. *Proc Natl Acad Sci U S A*. 2002; 99(25):16267–16272. [PubMed: 12444255]
94. Dodd SJ, Williams M, Suhan JP, Williams DS, Koretsky AP, Ho C. Detection of single mammalian cells by high-resolution magnetic resonance imaging. *Biophys J*. 1999; 76(1 Pt 1): 103–109. [PubMed: 9876127]
95. Shapiro EM, Sharer K, Skrtic S, Koretsky AP. In vivo detection of single cells by mri. *Magn Reson Med*. 2006; 55(2):242–249. [PubMed: 16416426]
96. Foster-Gareau P, Heyn C, Alejski A, Rutt BK. Imaging single mammalian cells with a 1.5 t clinical mri scanner. *Magn Reson Med*. 2003; 49(5):968–971. [PubMed: 12704781]
97. Sumner JP, Shapiro EM, Maric D, Conroy R, Koretsky AP. In vivo labeling of adult neural progenitors for mri with micron sized particles of iron oxide. Quantification of labeled cell phenotype. *Neuroimage*. 2009; 44(3):671–678. [PubMed: 18722534]
98. Shapiro EM, Gonzalez-Perez O, Manuel Garcia-Verdugo J, Alvarez-Buylla A, Koretsky AP. Magnetic resonance imaging of the migration of neuronal precursors generated in the adult rodent brain. *Neuroimage*. 2006; 32(3):1150–1157. [PubMed: 16814567]
99. Vreys R, Vande Velde G, Krylychkina O, Vellema M, Verhoye M, Timmermans JP, Baekelandt V, Van der Linden A. Mri visualization of endogenous neural progenitor cell migration along the rms in the adult mouse brain. Validation of various mpio labeling strategies. *Neuroimage*. 2010; 49(3):2094–2103. [PubMed: 19850132]
100. Zabow G, Dodd SJ, Moreland J, Koretsky AP. The fabrication of uniform cylindrical nanoshells and their use as spectrally tunable mri contrast agents. *Nanotechnology*. 2009; 20(38):385301. [PubMed: 19713581]
101. Zabow G, Dodd S, Moreland J, Koretsky A. Micro-engineered local field control for high-sensitivity multispectral mri. *Nature*. 2008; 7198; 453:1058–1063. [PubMed: 18563157]
102. Bendszus M, Ladewig G, Jestaedt L, Misselwitz B, Solymosi L, Toyka K, Stoll G. Gadofluorine m enhancement allows more sensitive detection of inflammatory cns lesions than t2-w imaging. A quantitative mri study. *Brain*. 2008; 131(Pt 9):2341–2352. [PubMed: 18669504]
103. Aoki I, Takahashi Y, Chuang KH, Silva AC, Igarashi T, Tanaka C, Childs RW, Koretsky AP. Cell labeling for magnetic resonance imaging with the t1 agent manganese chloride. *NMR Biomed*. 2006; 19(1):50–59. [PubMed: 16411253]
104. Vittorio O, Duce SL, Pietrabissa A, Cuschieri A. Multiwall carbon nanotubes as mri contrast agents for tracking stem cells. *Nanotechnology*. 2011; 22(9):095706. [PubMed: 21270482]

105. Bonetto F, Srinivas M, Heerschap A, Mailliard R, Ahrens ET, Figdor CG, de Vries IJ. A novel (19)f agent for detection and quantification of human dendritic cells using magnetic resonance imaging. *Int J Cancer*. 2010
106. Meng X, Seton HC, Lu LT, Prior IA, Thanh NT, Song B. Magnetic opt nanoparticles as mri contrast agent for transplanted neural stem cells detection. *Nanoscale*. 2011
107. Ahrens ET, Flores R, Xu H, Morel PA. In vivo imaging platform for tracking immunotherapeutic cells. *Nat Biotechnol*. 2005; 23(8):983–987. [PubMed: 16041364]
108. Srinivas M, Turner MS, Janjic JM, Morel PA, Laidlaw DH, Ahrens ET. In vivo cytometry of antigen-specific t cells using 19f mri. *Magn Reson Med*. 2009; 62(3):747–753. [PubMed: 19585593]
109. Wu YL, Ye Q, Ho C. Cellular and functional imaging of cardiac transplant rejection. *Curr Cardiovasc Imaging Rep*. 2011; 4(1):50–62. [PubMed: 21359095]
110. Jo SK, Hu X, Kobayashi H, Lizak M, Miyaji T, Koretsky A, Star RA. Detection of inflammation following renal ischemia by magnetic resonance imaging. *Kidney Int*. 2003; 64(1):43–51. [PubMed: 12787394]
111. Floris S, Blezer EL, Schreibelt G, Dopp E, van der Pol SM, Schadee-Eestermans IL, Nicolay K, Dijkstra CD, de Vries HE. Blood-brain barrier permeability and monocyte infiltration in experimental allergic encephalomyelitis. A quantitative mri study. *Brain*. 2004; 127(Pt 3):616–627. [PubMed: 14691063]
112. Stoll G, Bendszus M. New approaches to neuroimaging of central nervous system inflammation. *Curr Opin Neurol*. 2010; 23(3):282–286. [PubMed: 20168228]
113. Neuwelt EA, Varallyay CG, Manninger S, Solymosi D, Haluska M, Hunt MA, Nesbit G, Stevens A, Jerosch-Herold M, Jacobs PM, Hoffman JM. The potential of ferumoxytol nanoparticle magnetic resonance imaging, perfusion, and angiography in central nervous system malignancy. A pilot study. *Neurosurgery*. 2007; 60(4):601–611. discussion 611-602. [PubMed: 17415196]
114. Vellinga MM, Oude Engberink RD, Seewann A, Pouwels PJ, Wattjes MP, van der Pol SM, Pering C, Polman CH, de Vries HE, Geurts JJ, Barkhof F. Pluriformity of inflammation in multiple sclerosis shown by ultra-small iron oxide particle enhancement. *Brain*. 2008; 131(Pt 3): 800–807. [PubMed: 18245785]
115. Yeh TC, Zhang W, Ildstad ST, Ho C. In vivo dynamic mri tracking of rat t-cells labeled with superparamagnetic iron-oxide particles. *Magn Reson Med*. 1995; 33(2):200–208. [PubMed: 7707910]
116. Zhang F, Xie J, Liu G, He Y, Lu G, Chen X. In vivo mri tracking of cell invasion and migration in a rat glioma model. *Mol Imaging Biol*. 2010
117. de Vries IJ, Lesterhuis WJ, Barentsz JO, Verdijk P, van Krieken JH, Boerman OC, Oyen WJ, Bonenkamp JJ, Boezeman JB, Adema GJ, Bulte JW, et al. Magnetic resonance tracking of dendritic cells in melanoma patients for monitoring of cellular therapy. *Nat Biotechnol*. 2005; 23(11):1407–1413. [PubMed: 16258544]
118. Mueller SG, Schuff N, Yaffe K, Madison C, Miller B, Weiner MW. Hippocampal atrophy patterns in mild cognitive impairment and alzheimer's disease. *Hum Brain Mapp*. 2010; 31(9): 1339–1347. [PubMed: 20839293]
119. Shapiro MG, Westmeyer GG, Romero PA, Szablowski JO, Kuster B, Shah A, Otey CR, Langer R, Arnold FH, Jasanoff A. Directed evolution of a magnetic resonance imaging contrast agent for noninvasive imaging of dopamine. *Nat Biotechnol*. 2010; 28(3):264–270. [PubMed: 20190737]
120. Jasanoff A. Mri contrast agents for functional molecular imaging of brain activity. *Curr Opin Neurobiol*. 2007; 17(5):593–600. [PubMed: 18093824]

A. in-vivo MRI

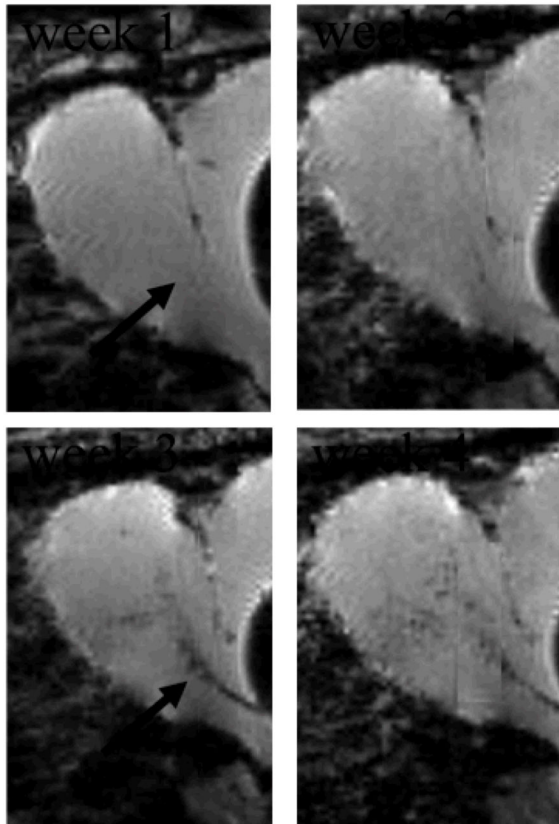


B. post-mortem histology and MRI

**Fig 1.**

a. Anatomical detail in human brain visualized by in vivo MRI at 7T. Magnetic susceptibility induced frequency contrast allows visualization of layer 4b (line of Gennari) of the primary visual cortex (white arrow) and the main white matter fibers of the optic radiation (black arrow) that connect to it. Resolution: $200 \times 200 \times 1000 \mu\text{m}$. b,c. iron stain and MRI transverse relaxivity (R_2^*) image, demonstrating the colocalization of areas with increased iron content and increased relaxivity (arrows)

A. Migrating progenitors



B. Single cells in olfactory bulb.

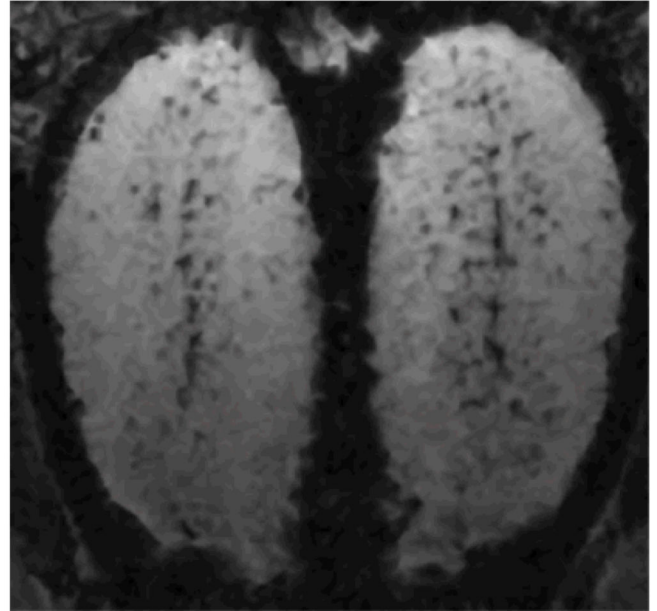


Fig 2.

MRI detection of the migration of endogenous neural precursors along the rostral migratory stream (A) to the olfactory bulb (B) of the rat. Micron-size particles of iron oxide were directly injected into the ventricle near the subventricular zone where new neural precursors are continually generated. Over the course of a few weeks signal loss due to cell migration from precursors that have taken up iron oxide particles can be clearly seen as dark spots along the rostral migratory stream (arrow). Three weeks after injection many dark punctuate spots can be detected throughout the olfactory bulb (B) which correspond to single cells that have migrated into the bulb. (Adopted from [97,98])